ARTICLE | OPEN ACCESS

Indian journal of
Engineering

To Cite:
Salih MK, AbdulRazzaq GH, Humadi JI. Synergistic (Fe_2O_3 + NiO) /Alumina Catalyst for Hydrogen Peroxide-Based Oxidative Desulfurization of Petroleum Fuel under Ultrasonic Irradiation: Kinetic and Catalytic Study. *Indian Journal of Engineering*, 2026, 23, e11ije1728
doi:

Author Affiliation:
Petroleum and Gas Refining Engineering Department, College of Petroleum Processes Engineering, Tikrit University, Tikrit 34001, Iraq

ORCIDs:
Mohammed K. Salih: https://orcid.org/0009-0005-1993-3067
Ghassan Hassan AbdulRazzaq: https://orcid.org/0000-0002-2975-168X
Jasim I. Humadi: https://orcid.org/0000-0002-7597-2635

Corresponding author:
Jasim I. Humadi,
Petroleum and Gas Refining Engineering Department, College of Petroleum Processes Engineering, Tikrit University, Tikrit 34001, Iraq
E-mail: jasim_alhashimi_ppe@tu.edu.iq

Peer-Review History
Received: 18 October 2025
Reviewed & Revised: 21/November/2025 to 03/August/2026
Accepted: 21 August 2026
Published: 05 September 2026

Peer-Review Model
External peer-review was done through double-blind method.

Indian Journal of Engineering
pISSN 2319–7757; eISSN 2319–7765

DISCOVERY
SCIENTIFIC SOCIETY

Synergistic (Fe_2O_3 + NiO)/Alumina Catalyst for Hydrogen Peroxide-Based Oxidative Desulfurization of Petroleum Fuel under Ultrasonic Irradiation: Kinetic and Catalytic Study

Mohammed K Salih, Ghassan Hassan AbdulRazzaq, Jasim I Humadi*

ABSTRACT

To achieve a clean, pollution-free environment, given the health and environmental hazards of sulfur, it is essential to identify effective methods for reducing its concentration to the lowest internationally permissible levels. Many methods have emerged to achieve this, but they have numerous drawbacks, whether financial, economic, or hazardous. From this perspective, oxidative desulfurization (ODS) technology has emerged, operating under moderate and less hazardous conditions. Therefore, it has become necessary to develop suitable catalysts for this technology to effectively remove sulfur compounds from fuels. This research paper discusses the preparation of a catalyst from (Fe_2O_3 + NiO)/ γ-Al_2O_3. The following tests were performed: Brunauer-Emmett-Teller (BET), X-ray diffraction (XRD), energy-dispersive X-ray (EDX), Thermal gravimetric analysis (TGA), and scanning electron microscopy (SEM) to validate the catalyst preparation. The efficiency of the catalyst prepared in an ultrasonic reactor was also evaluated in the oxidative desulfurization (ODS) process for removing sulfur compounds from diesel fuel in the presence of an oxidizing agent. Using different temperatures (25-75°C) and different reaction times (30_60) minutes for diesel, with sonication intensities (80%-90%-100%), the best sulfur compound removal rate from diesel after extraction by ethanol reached 91%. Under optimal conditions, the temperature was 75°C, the reaction time was up to 60 minutes, and the sonication intensity was 100%. The reaction order and activation energy were also evaluated, showing that it tends towards pseudo-first-order and has an activation energy of 18 kJ/mol.

Keywords: Oxidative desulfurization (ODS), diesel fuel, catalyst preparation, bimetallic catalyst, ultrasonic reactor, sulfur removal.

1. INTRODUCTION

With the world's industrial and technological advancements, there has been a significant increase in energy sources recently to meet growing demand. Since fossil fuels constitute 90% of energy sources, the demand for them has increased dramatically (Haruna et al., 2025). The ever-increasing demand for energy has made crude oil one of the most important energy sources; therefore, global agencies predict that by 2040, the demand for energy and fossil fuels could increase by 30% (Mohammed et al., 2025). One of the most significant industrial problems and obstacles affecting the environment is the sulfur compounds found in fuels, specifically thiophene and dibenzothiophene, which negatively impact the environment (Beshtar et al., 2025). Sulfur compounds are considered the primary cause of respiratory problems, acid rain, air pollution, soil problems, heart disease, and asthma. They also lead to catalyst contamination in industrial processes, corrosion of refining equipment, and problems with car engines (Jafar et al., 2021; Wu et al., 2025).

Because of the harmful effects of sulfur pollution, countries have enacted strict laws to limit sulfur emissions and promote cleaner fuels. Environmental laws have set permissible limits for sulfur content in fuel between 10–15 parts per million, intending to reduce sulfur levels and limit its effects on the environment (Hossain et al., 2019). Therefore, in compliance with accepted environmental requirements, efficient methods should be used to lower the sulfur level in petroleum derivatives. One of the leading processes in this area is HDS technology, which reduces sulfur content. However, it has several drawbacks that make it unsuitable for this purpose. These drawbacks include operating at very high temperatures (300-400°C) and very high hydrogen pressure (3-6 MPa), as well as a limited ability to remove aromatic sulfur compounds such as DBT (Mohammed and Jarullah, 2023). Given all these drawbacks, an alternative to HDS technology is necessary. We understand that there are several alternative technologies for removing sulfur compounds, including biological (Davoodi-Dehaghani et al., 2010; Dinamarca et al., 2010; Bhasarkar et al., 2015), adsorption (Jiang et al., 2003; Ahmed and Ahmaruzzaman, 2015; Miao et al., 2015), electrochemical desulfurization (Tavan et al., 2020), extraction (Mohammed et al., 2015; Zuraiqi et al., 2018), and oxidative processes (Jafar et al., 2021; Kayedi et al., 2021; Mohammed et al., 2025; Beshtar et al., 2025; Haruna et al., 2025; Wu et al., 2025). Among these technologies, ODS technology is currently the most promising and important for researchers, as it possesses several advantages that qualify it for this role. These include its ability to operate under moderate temperature and pressure conditions, its lack of reliance on expensive hydrogen gas, and its capacity to remove stubborn sulfur compounds compared to HDS technology (Alwan et al., 2020; Salem et al., 2025). The ODS technology works by oxidizing the sulfur compounds present in diesel by adding oxygen molecules, converting them into sulfoxides and sulfonates (Zhang et al., 2009). The oxidation process relies on oxidants to provide oxygen to complete the process, and many oxidants have been used, such as O_2 (Mohammed et al., 2025), H_2O_2 (de Luna et al., 2018), air (Jarullah et al., 2020), TPHB (Chica et al., 2006), t-BuOOH (Ishihara et al., 2005).

The oxidation process is carried out using different catalysts, and researchers have used many catalysts, including Fe_2O_3/Gr (Alwan et al., 2020), V_2O_5/TiO_2 (Cedeno-Caero et al., 2008), and HPW/AC (Barilla *et al*., 2022). Many researchers have also focused on using alumina-supported catalysts, such as ZnO/γ-Al_2O_3 (Nawaf et al., 2019), MgO+ ZnO/ γ-Al_2O_3 (Abdulateef et al., 2018), MoO_3/γ-Al_2O_3 (Jia et al., 2011). Alumina is considered an excellent support material because it provides good surface area, excellent porosity, and an even distribution of the active metal without clumping. It also withstands temperature fluctuations without being affected. All these features help it effectively remove sulfur, especially DBT (Jia et al., 2011; Beshkoofeh et al., 2021; Al-Tabbakh and Jarullah, 2023; Özcan and Akın, 2025). Thus, the synthesis of an Fe_2O_3–NiO/γ-Al_2O_3 catalyst for hydrogen peroxide-based oxidative desulfurization under ultrasonic irradiation, using the incipient wetness impregnation approach, is the focus of this work. This work is innovative in that it examines the efficacy of sulfur removal by combining ultrasonic-assisted oxidation, a bimetallic catalyst, and kinetic assessment.

2. METHODOLOGY AND EXPERIMENTAL MATERIALS

Chemical materials and fuel

Diesel feedstock containing sulfur at 2018.14 ppm was obtained from North Refineries Company. The physical properties of the diesel are shown in Table 1. The alumina, prepared locally from the following materials: Aluminum Nitrate ($Al(NO_3)_3.9H_2O$) with a purity of 98%, was obtained from LOBA CHEMIE PVT.LTD. Ammonium hydroxide (NH_4OH) with a purity of 99.9% from RCI LABSCAN LIMITED was used, along with 25% purity ethanol (C_2H_5OH) from RCI LABSCAN LIMITED and deionized water. The materials used during metal loading onto the support were Nickel(II) Nitrate Hexahydrate ($Ni(NO_3)_2.6H2O$) with a purity of 99% from Central Drug House (CDH) and Ferric Nitrate Nonahydrate ($Fe(NO_3)_3.9H2O$) with a purity of 98% from Central Drug House (CDH). The oxidizing agent used was hydrogen peroxide (H_2O_2) with a purity of 35% obtained from PanReac AppliChem. Oxidation is used to convert sulfur compounds into sulfoxides and sulfones.

Table 1. Physical properties of diesel

PHYSICAL PROPERTY	DIESEL
SP.GR@15.6	0.8217
FLASH POINT	62
TOTAL SULFUR (PPM)	2018.14
API GRAVITY	40.7
VISCOSITY (SCT) @ 40 ℃	3.15
COLOUR	0.9
DISTILLATION	
I.B.P ℃	175
5%	183
10%	190
50%	252
90%	320
95%	338
EP%	354

Preparation of the catalyst

Preparation of γ-Al_2O_3 support

The gamma-alumina support was prepared using a chemical reaction. 80 g of aluminum nitrate was added to a glass beaker, followed by 100 ml of deionized water. The mixture was then placed on a magnetic stirrer until it dissolved and was thoroughly mixed. Aluminum hydroxide was gradually added to the mixture until a gel formed at pH 7. After that, the material underwent a washing process using deionized water and ethanol to remove impurities; then the liquids were removed, and the material was dried. A drying oven was used at 120°C for 12 hours to remove the water from the sample; then it was roasted at 200°C for one hour, at 400°C for one hour, and finally it was stabilized at 600°C for 4 hours. It was allowed to cool to room temperature and then finely ground. Fig.1 illustrates the process details.

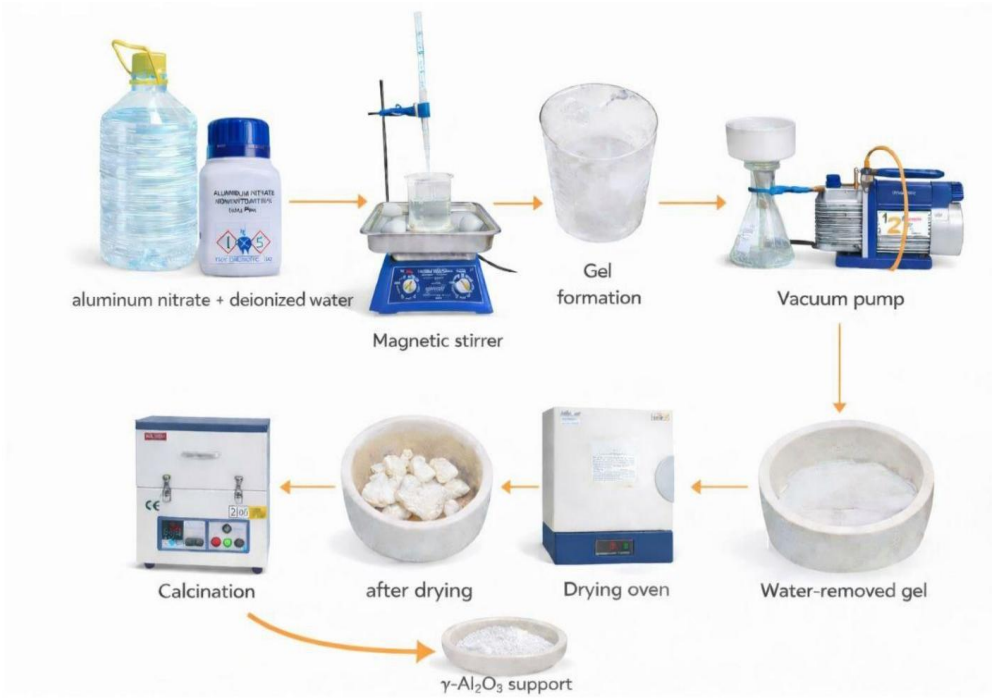

Figure 1. Manufacturing steps of γ-Al_2O_3 support

Preparation of (Fe_2O_3 + NiO) /γ-Al_2O_3

The catalyst is prepared using the incipient wetness impregnation (IWI) method. Three grams of $Fe(NO_3)_3.9H_2O$ are dissolved with two grams of $Ni(NO_3)_2.6H_2O$ in 80 mL of deionized water. The mixture is thoroughly mixed for 1 hour using a magnetic stirrer, followed by another hour of ultrasonic mixing. 6 gm of alumina is then added and mixed thoroughly. The mixture is dried overnight at 120°C in a drying oven for 12 hours, calcined at a temperature of 200 for 1 hour, then at 400 for 1 hour, and finally stabilized at a temperature of 600 for 4 hours, then calcined at 600°C in a tubular furnace. Finally, it was ground to form the catalyst, as shown in Figure 2.

On a γ-Al_2O_3 substrate, the prepared catalyst has a nominal loading of 5% weight percent iron and 5% nickel. The catalytic efficacy of the Fe–Ni catalyst under ultrasonic oxidative desulfurization conditions was assessed using this stable binary structure. Instead of optimizing the Fe/Ni ratio or the total metal loading, the current work sought to examine the effects of reaction temperature, reaction duration, and ultrasonic intensity as well as the kinetic behavior of the selected catalytic arrangement. As a result, the configuration examined in this study is 5 weight percent Fe – 5 weight percent Ni; it is not considered the ideal design. Future studies aiming to enhance catalyst design may examine various Fe/Ni ratios and metal loadings.

Figure 2. shows the steps of the catalyst.

Catalyst characterization

The prepared catalyst (Fe_2O_3 + NiO)/γ-Al_2O_3 was studied and tested using various instruments, including X-ray diffraction (XRD) and Measurement Temperature 25°C and Start Position [°2Th.] 9.3860 and End Position [°2Th.] 79.9860, Brunauer, Emmett, and Measurement Temperature 120C for 2hour Teller (BET) Adsorptive by N_2 and Adsorption cross section area is 0.162 [nm^2], and scanning electron microscopy (SEM).

Oxidative Desulfurization Procedure

The performance of the catalyst (Fe_2O_3 + NiO)/γ-Al_2O_3 was evaluated in the ODS technique using the ultrasonic reactor (Made by a Chinese company) shown in Fig. 3. Diesel containing total sulfur compounds of 2018.14 ppm was used with the oxidizing agent H_2O_2. For each run, 20 ml of diesel was fed with 2 ml of H_2O_2 and 0.5 g of the catalyst at atmospheric pressure. The performance of the catalytic system was assessed in this investigation using a fixed dosage of H_2O_2 under authorized operating conditions. The ratio of H_2O_2 to sulfur content was not examined as a separate variable. The amount of hydrogen peroxide (H_2O_2) used can affect the economic efficiency of the process if it exceeds the specified proportions, and it may also negatively impact the oxidation process with adverse results. Excessive use does not necessarily lead to a higher desulfurization rate. Thus, optimizing oxidizer use and evaluating the system's viability in further research depend on figuring out the ideal H_2O_2-to-sulfur content ratio. The catalyst dose was not investigated as an independent variable in the current trials, and the quantity of catalyst was set at 0.5 g per 20 mL of diesel fuel. Nevertheless, adding more catalyst can increase the number of active sites available for $H2O_2$ activation and sulfur compound

oxidation, but doing so too much could not result in a commensurate increase in removal efficiency. As a result, figuring out the ideal catalyst dose is essential for striking a balance between catalytic activity, catalyst consumption, and separation needs. It is also a recommended strategy for enhancing the procedure in future research.

The oxidation process was carried out under moderate conditions, at temperatures of (25-75 °C), with reaction times of (30_60) minutes, and mixing speeds in the ultrasonic system (80-100%). After the oxidation process and the conversion of sulfur to sulfoxides and sulfonates, the catalyst is then separated using 9 cm filter paper. The sulfoxides and sulfonates are more polar, so they are dissolved with a polar solvent (ethanol) in a 1:1 ratio, thus obtaining diesel fuel with low sulfur content. The ethanol extraction stage is an essential component of the oxidative desulfurization process, which aims to remove the more polar sulfur oxidation products from the hydrocarbon phase following treatment. The high efficiency achieved is due to the combined oxidation and extraction processes, which are interconnected in this work. Extraction alone, without oxidation, was not tested, although this is necessary in future experiments and processes to determine the efficiency and effects of each process individually and to define the contribution of each. The diesel is then separated from the polar solvent, and the sulfur content is analyzed using a Sindy apparatus manufactured in the United States by XOS. This apparatus utilizes the principle of single-wavelength X-ray scattering (MWDXRF) technology and is considered one of the most accurate methods for determining total sulfur content. The device operates according to ASTM D7039 standards for determining total sulfur content. It is crucial to remember that genuine, unpolluted diesel fuel was used in this study's desulfurization performance evaluation rather than a model fuel made in a lab. Additionally, the desulfurization assessment was predicated on determining the sample's total sulfur content both before and after treatment using a widely accessible sulfur analyzer, which yields a number for the overall sulfur content but does not distinguish specific sulfur species. As a result, the computed desulfurization efficiency values in this study do not allow for the assessment of the individual contribution of various sulfur species; instead, they represent the total reduction in sulfur concentration. Identifying specific species, such as dibenzothiophene (DBT) and its derivatives, 4,6-DMDBT, and thiophene, could offer a more thorough understanding of the selectivity and behavior of the ODS process because the susceptibility of sulfur compounds to oxidation and removal varies according to their molecular structure. Therefore, while the current results clearly reflect the total desulfurization effectiveness of the actual diesel fuel under research, qualitative and quantitative characterization of specific sulfur species using specialist analytical techniques constitutes an essential expansion of the current work.

The desulfurization efficiency was also calculated using Eq.1

$$convegen\ \% = \left(1 - \frac{CA_{IN} - CA_{OUT}}{CA_{IN}}\right) \times 100\% \ldots\ldots\ldots\ldots\ldots\ldots\ldots\ldots\ldots 1$$

Where, CA_{IN} is the initial concentration, CA_{OUT} is the final concentration of sulfur measured in parts per million (ppm).

Figure 3. Ultrasonic Reactor.

3. RESULTS & DISCUSSIONS

Catalyst characterization

Surface area and pore volume analysis

The surface area, pore volume, and diameter of the prepared catalyst (Fe_2O_3 + NiO)/γ-Al_2O_3 were examined using the Brunauer-Emmett-Teller (BET) test, as shown in Table 2. The results showed that the surface area of the gamma-alumina catalyst before metal loading was larger, and after loading iron and nickel, the surface area decreased. This indicates that the pores were filled with metal (Ahmed et al., 2020). The pore volume and diameter also decreased after metal loading. This surface area is considered excellent for gamma-alumina in its neutralized form, as it is effective in completing the desulfurization reaction**.** The BET curves for γ-Al_2O_3 and for (Fe2O3 + NiO)/γ-Al_2O_3 are shown in Figure 4A and B, respectively.

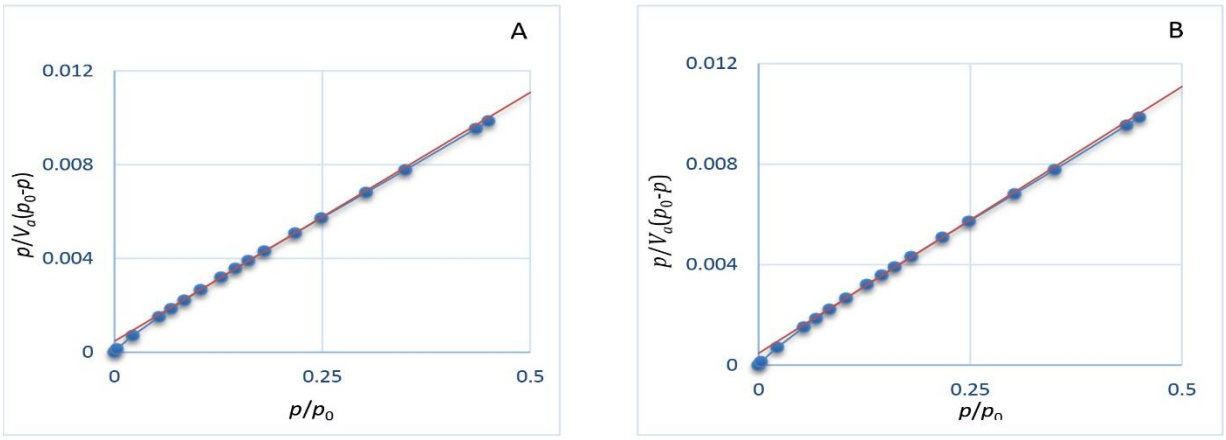

Figure 4. BET OF (A) γ-Al_2O_3 & (B) OF (Fe_2O_3 + NiO) /γ-Al_2O_3

Table 2. results of BET

Sample	Surface area(m^2/g)	Mean pore diameter (nm)	Total pore volume (cm^3/g)
γ-Al_2O_3	216.99	6.133	0.3327
(Fe_2O_3 + NiO) /γ-Al_2O_3	200.73	4.5715	0.2294

X-ray diffraction (XRD)

X-ray diffraction (XRD) results for the prepared γ-Al_2O_3 material, as shown in Fig. 5A, within the 2θ-angle range of 9.38–79.98° and a 0.05° scan line using a wavelength of λ = 1.5406 Å and Cu Kα radiation, revealed a diffraction pattern exhibiting broad main peaks at 2θ ≈ 37.8°, 45.1°, and 66.1°, where these values correspond to the gamma alumina phase (Hosseini et al., 2012; Khazaei et al., 2016; Sobhani and Tavakoli, 2019; Jarullah et al., 2022) .The peaks also indicate the formation of nano-sized γ-Al_2O_3. The average crystal size was also calculated using the Debye-Scherrer equation (Rayalu et al., 2005).

$$D = \frac{K\lambda}{\beta \cos\theta}$$

Where D is the diameter of the crystallite, k = 0.9, λ is the wavelength of the X-ray, β full width at half maximum (FWHM), and θ is the diffraction angle. The average crystal size of the γ-Al_2O_3 sample was calculated using the equation above. At the highest intensity of 2θ = 66.0° and at (FWHM) 7.93°, the crystal size was approximately 1.2 nm, confirming the nanoscale nature of the prepared gamma alumina. Fig.5B shows the XRD scan of the prepared scaffold after metal loading (Fe_2O_3 + NiO) /γ-Al_2O_3. The active catalyst is observed to integrate with the prepared γ-Al_2O_3 peaks, indicating high metal dispersion and the absence of clumping on the scaffold or the formation of very fine crystals that were not detected by XRD (Zeifert et al., 2000; Mangesh et al., 2024). This high dispersion is common for metals and is beneficial in catalytic applications for enhancing the interactions between the prepared scaffold and the metal.

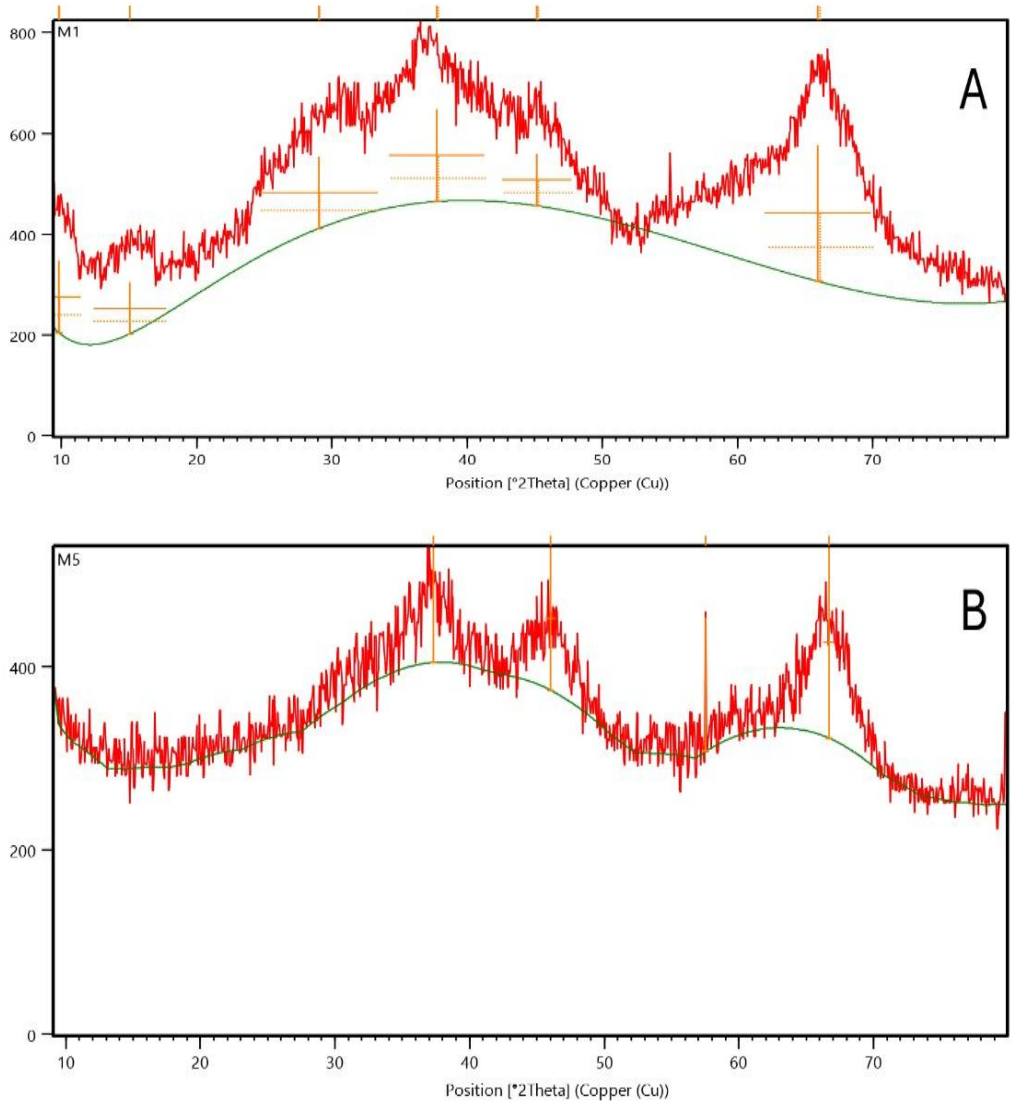

Figure 5. XRD patterns for synthesized (A) γ-Al_2O_3 & (B) OF (Fe_2O_3 + NiO) / γ-Al_2O.

Thermal gravimetric analysis (TGA)

The thermal behavior of γ-Al_2O_3 and Fe_2O_3 + NiO / γ-Al_2O_3 was examined using thermogravimetric analysis (TGA) in an argon environment. As shown in Fig. 6A, B. At 600 °C, the Fe_2O_3 + NiO / γ-Al_2O_3 catalyst lost 24.96 wt.% of its weight, compared to 17.64 wt.% for γ-Al_2O_3. Fig. 6A illustrates the weight loss that occurs below 120°C due to the removal of physically absorbed water on the outer surface and within the pore structure of γ-Al_2O_3 (Kozerozhets et al., 2023). The increasing condensation of hydrogen-bonded surface hydroxyl groups and the elimination of highly adsorbed water are linked to the gradual mass loss between about 120 and 350 °C (Ludwig and Burke, 2022). The significant weight loss at 350°C is attributed to the removal of hydroxyl groups (Al-OH-Al), which may contribute to the formation of symmetrical unsaturated alumina subsites, consistent with the behavior of gamma alumina (Ma et al., 2024). Fig. 6B: After Fe_2O_3 and NiO loading, the larger overall weight loss is attributable to the alteration of the alumina surface produced by metal–support interaction, which increases the quantity of adsorbed water and surface hydroxyl species maintained at the metal–support interface. As a result, when heated in an inert environment, dehydration and dehydroxylation become more noticeable, although Fe_2O_3 and NiO themselves stay thermally stable below 600 °C (Wang et al., 2023; Ma et al., 2024).

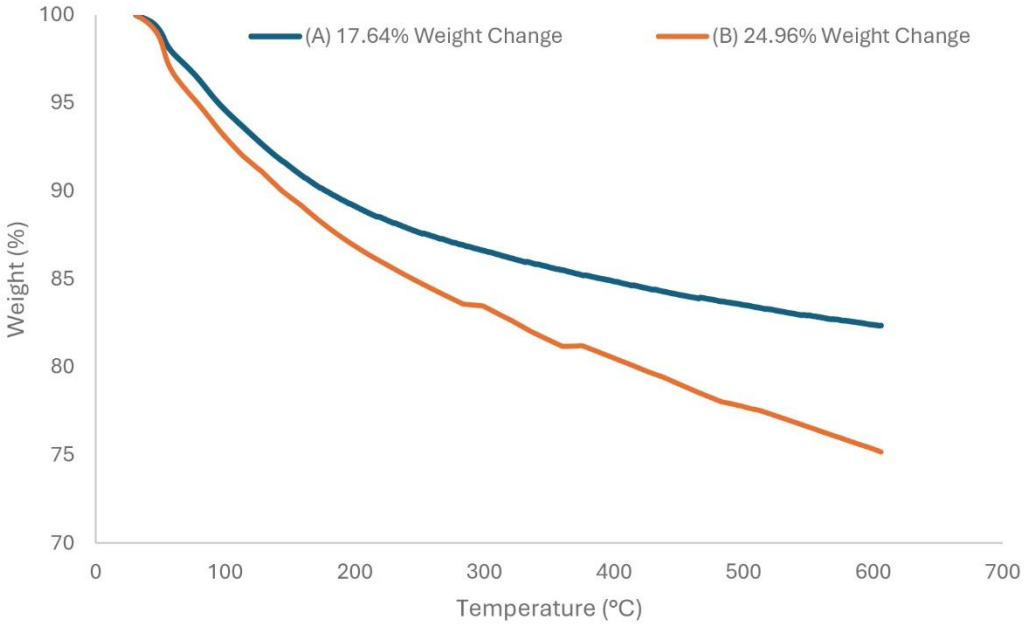

Figure 6. TGA for synthesized (A) γ-Al_2O_3 & (B) OF (Fe_2O_3 + NiO) / γ-Al_2O

Energy Dispersive X-ray (EDX)

The locally prepared material was analyzed using Energy Dispersive X-ray (EDX). This assay was used to analyze and identify the material's constituent elements and assess its purity. The EDX spectrum showed distinct peaks from aluminum (Al Kα at KeV = 1.5) and oxygen (O Kα at KeV = 0.52), confirming the successful formation of aluminum oxide, as shown in Fig. 7A. The absence of other significant peaks for other elements indicates that the prepared material possesses a high degree of purity. These results suggest that the prepared material consists primarily of aluminum and oxygen, which is consistent with the expected composition of aluminum oxide.

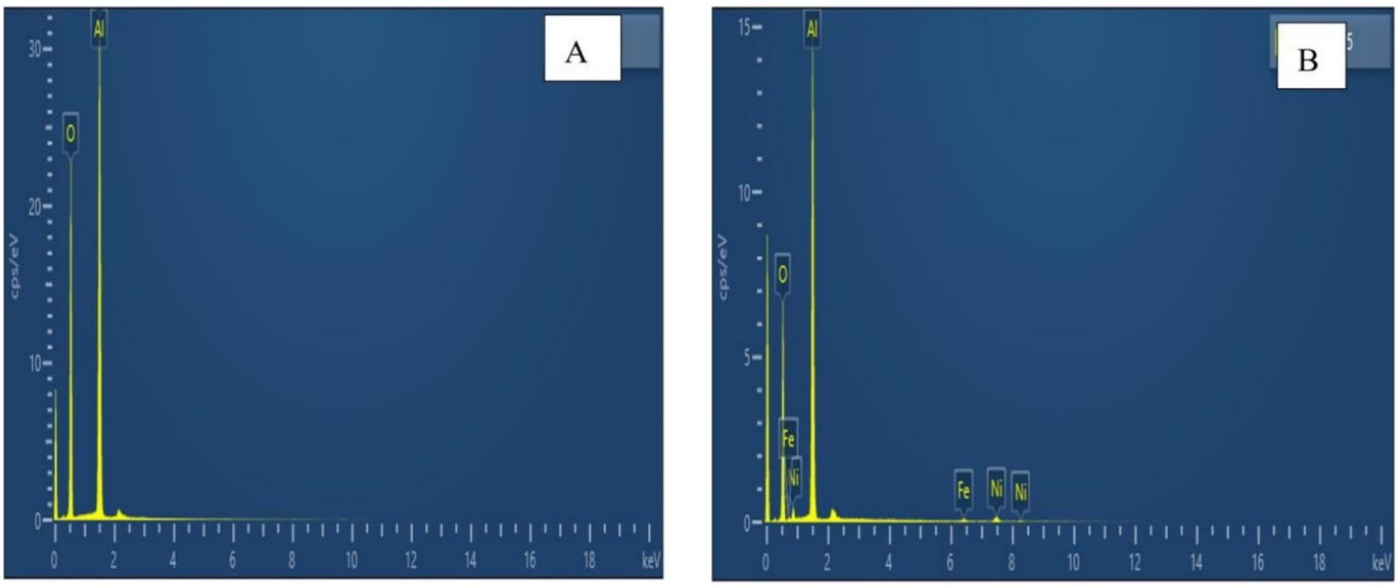

Figure 7. EDX OF(A) γ-Al_2O_3 & (B) OF (Fe_2O_3 + NiO) / γ-Al_2O_3

The EDX spectrum of (Fe2O3 + NiO)/γ-Al2O demonstrates the successful loading of the metals (iron and nickel) onto the alumina support, as illustrated in the figure 7. Peaks for iron are clearly observed at energies approaching 0.7, 6.4, and 7 kV, while peaks for nickel are observed at energies approaching 0.85, 7.5, and 8.2 kV. In addition to the actual peaks for alumina and oxygen, this indicates that the alumina support retains its structure and integrity after metal loading.

Scanning electron microscopy (SEM)

Scanning electron microscopy (SEM) was used to determine the surface morphology of the prepared material before and after metal loading. Fig.8A, B show the surface of the γ-Al_2O_3 support before metal loading, exhibiting irregularly shaped clusters of fine particles at the nanoscale, along with the appearance of agglomerates of the prepared alumina. The surface appears rough and porous. Fig.8C, D illustrates the significant difference in the support after metal loading (Fe_2O_3 + NiO) / γ-Al_2O_3, showing a rougher surface with a higher density of granular structures. These morphological changes confirm the successful loading of iron and nickel onto the alumina support. The paste-like particles are distributed at the nanoscale with good homogeneity across the support, and the porous structure remains largely intact with only minor changes.

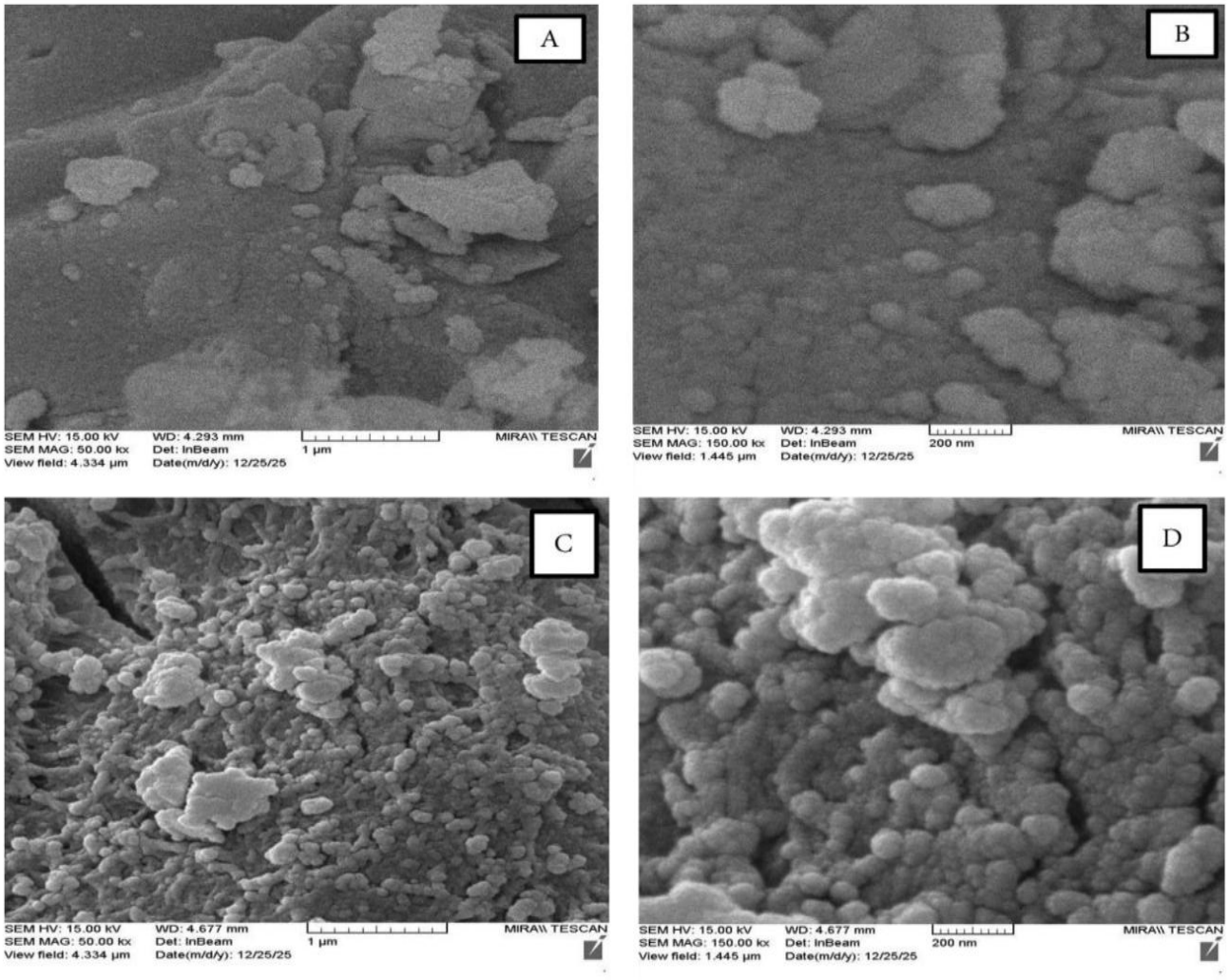

Figure 8. Scanning electron microscopy images of (A, B) γ-Al_2O_3 and (C, D) of (Fe_2O_3 + NiO) / γ-Al_2O_3

Oxidative desulfurization performance

Effect of ultrasonic temperature

Temperature is one of the most important factors that strongly influence the oxidative desulfurization process. Fig. 9(A-C) illustrates the effect of temperature changes on desulfurization efficiency. A reaction time of 60 minutes was used with an ultrasonic mixing

efficiency of (80%-100%). The results of the desulfurization tests showed that the removal efficiency increased with increasing temperature. This is attributed to several reasons, including the fact that as temperature increases, the proportionality constant increases, which in turn leads to increased sulfur removal efficiency according to the Arrhenius equation (Huang et al., 2017). Based on the Arrhenius equation, the reaction rate constant increases with increasing temperature. This, in turn, leads to an increase in the removal rate. Since the activation energy of the molecules depends on the reaction rate constant, increasing the activation energy of the molecules leads to a significant increase in the number of molecules participating in the reaction, thus increasing the removal efficiency (Nawaf et al., 2019). The calcination temperature of the prepared γ-Al_2O_3 material may also affect the acid site density, thereby increasing the removal rate (Jarullah et al., 2022).

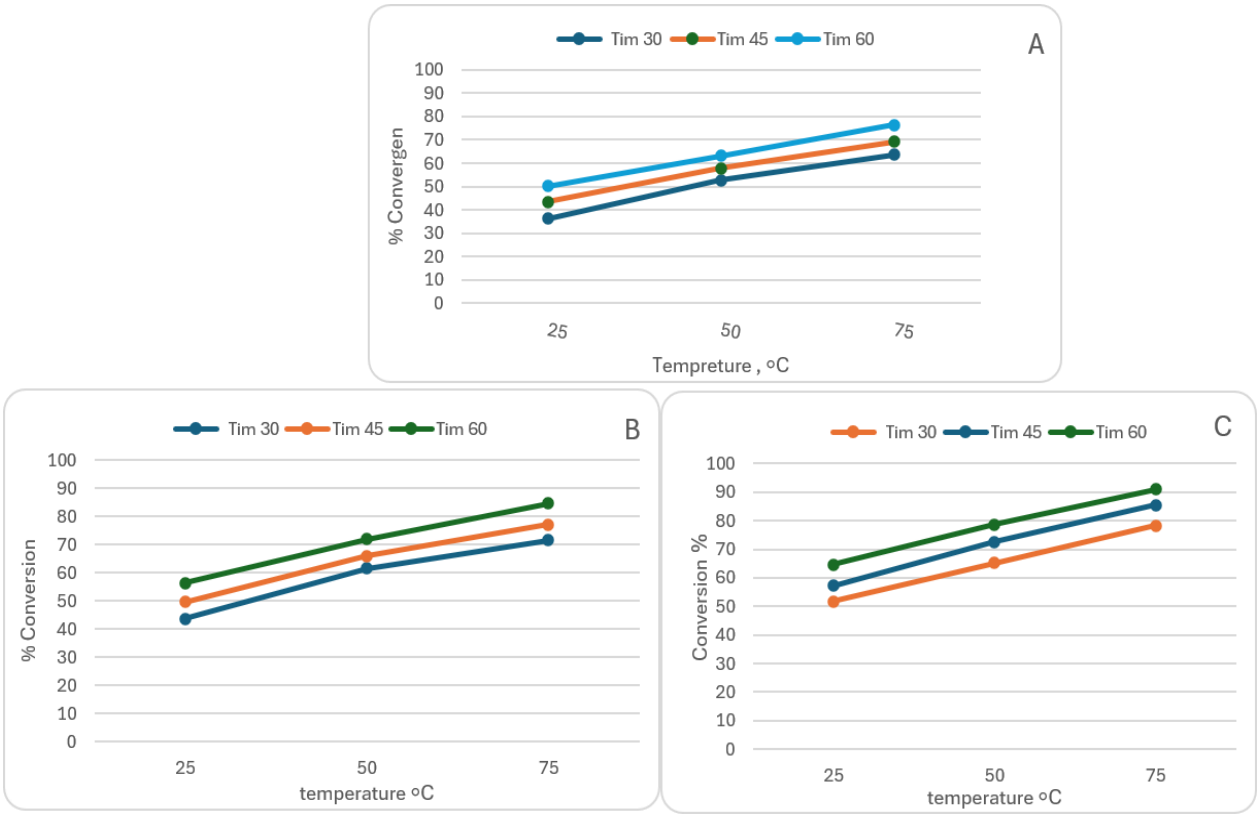

Figure 9. shows desulfurization in ODS technology with temperature variations according to ultrasonic efficiency: (A) 80%, (B) 90%, (C) 100%

Effect of reaction time in ultrasonic

Increasing the reaction time in ultrasonic mixing positively affects ODS desulfurization, as shown in Fig. 10(A, B, C) for operating times of 30,45 and 60 minutes with a temperature range of 25–75°C and an ultrasonic efficiency of 80%–100%. This increase in reaction time is due to the longer contact time between the reactants and the catalyst, which accelerates their oxidation in the presence of the oxidizing agent (Jafar et al., 2021; Nawaf et al., 2021; Humadi et al., 2023b). Furthermore, the increased reaction time allows for greater mass transfer, leading to enhanced reaction between the reactants and consequently a higher desulfurization rate (Fathi et al., 2022; Aabid et al., 2023; Humadi et al., 2023a; Razzaq et al., 2023; Algawi et al., 2024). The optimal desulfurization rate was achieved at 60 minutes, a temperature of 75°C, and 100% ultrasonic mixing intensity.

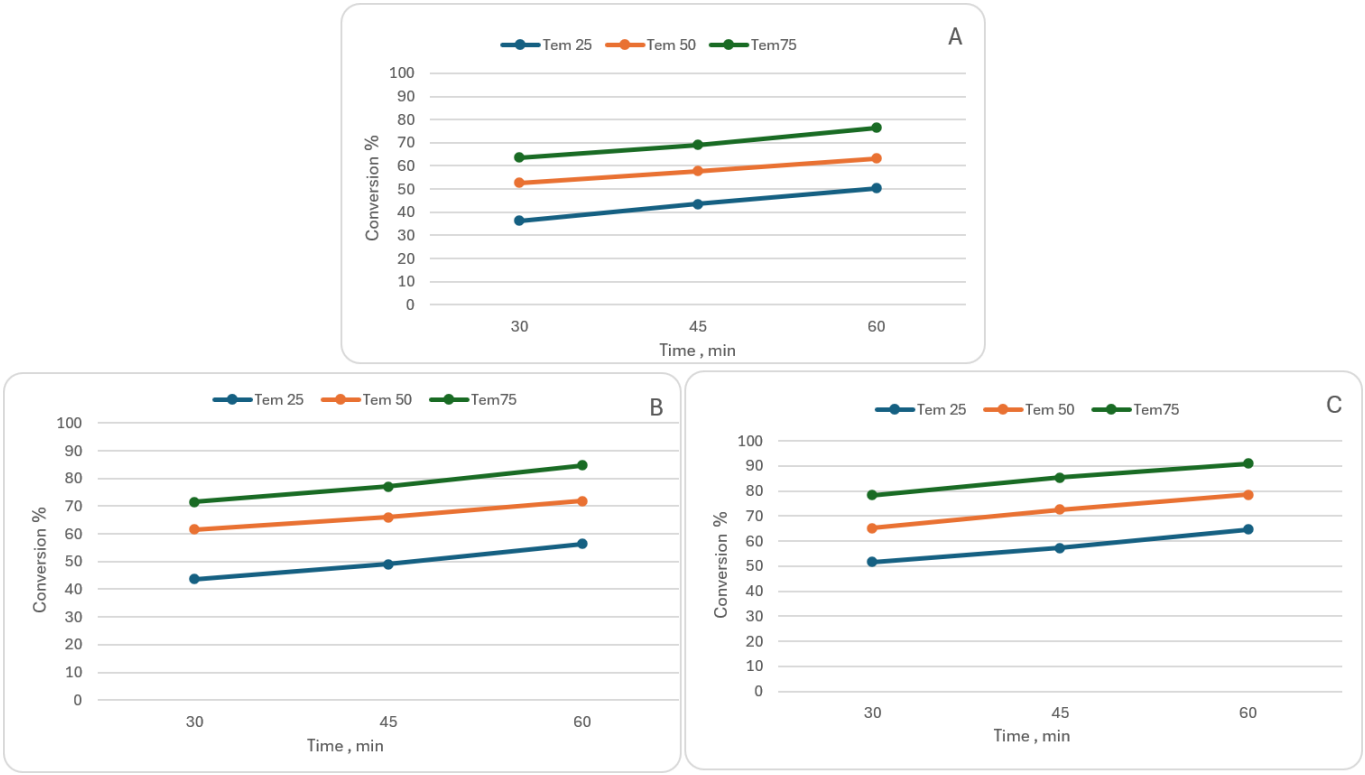

Figure 10. Shows desulfurization in ODS technology with reaction time variations according to ultrasonic efficiency: (A) 80%, (B) 90%, (C) 100%

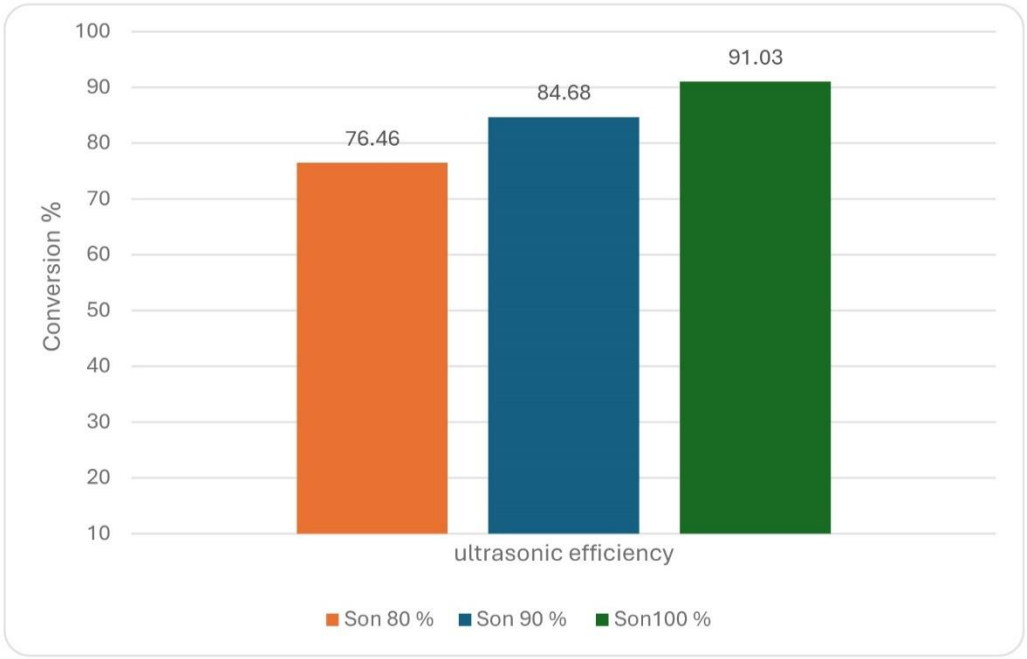

Figure 11. Shows desulfurization in ODS technology with Sonication intensity at a reaction time of 60 min and a temperature of 75◦C

Effect of Sonication Intensity

Fig.11 shows the effect of ultrasound on the ODS process at 75°C for 60 minutes across wave intensities of 80%, 90%, and 100%. The findings shown that when ultrasonic intensity increases, desulfurization efficiency rises. This is explained by the ultrasonic probe's

ability to improve reaction kinetics by increasing the dispersion of system components. Increased mass transfer between the solid and liquid phases as a result of mechanical and physical interactions is also credited with this improvement (Humadi et al., 2023a). The influence of ultrasound, which creates emulsification and acoustic cavities and improves contact between the diesel fuel, catalyst, and oxidizing agent, also affects process performance. As ultrasonic intensity increases, the desulfurization rate rises (Aabid et al., 2023). The highly catalytic Fe-Ni binary system contributes to the complementary properties of both, in addition to their effective role in H_2O_2 activation, as indicated by research such as (Ye et al., 2025). The connection between the two metal centers is crucial for increasing catalytic activity, since other research has shown that adding Fe to Ni sites can change the activation behavior of H_2O_2 and encourage the generation of reactive oxygen species (Martín et al., 2023). Fe_2O_3 and NiO combined on γ-Al_2O_3, as well as the metal components' superior dispersion and the improved fuel-oxidant interaction brought about by ultrasonic cavitation, can all contribute to the present system's increased oxidation of sulfur compounds. The integration of the Fe–Ni metal centers, the function of the support, and the enhancement of mass transfer under the influence of ultrasound are therefore responsible for the catalyst's improved performance. It should be noted that independent comparative experiments for individual catalysts are necessary to demonstrate direct chemical synergy between Fe and Ni.

Kinetic analysis of ODS Reactions

Two popular kinetic models for ODS reactions—the pseudo-first-order and pseudo-second-order models were investigated to ascertain the reaction rate and the underlying mechanism of ultrasonic oxidative desulfurization (UAODS) utilizing a nano-catalyst (Fe_2O_3 + NiO) / γ-Al_2O_3. The mathematical formulas for these two models are given by equations (2) and (3), respectively.

$$\ln(c_o - c_t) = k_1 t \dots\dots (2)$$

$$\frac{1}{c_t} - \frac{1}{c_o} = k_2 t \dots\dots (3)$$

Where:

c_o: represents the initial concentration of sulfur (ppm), ct: Sulfur concentration at time (t) (ppm), t: time (min), k_1: the rate constant for the first-order model (min^{-1}), k_2: the rate constant for the second-order model (ppm^{-1}. min^{-1}).

For both models, the kinetics were carried out at the maximal sonication intensity (100%), which is thought to be ideal, with varying response durations (30, 45, and 60 minutes) and temperatures (25, 50, and 75 °C). The first-order findings are shown in Fig. 12(A, B, C), and the second-order results are shown in Fig.13(A, B, C). With correlation coefficients (R^2) more than 0.99, the pseudo-first-order model demonstrated outstanding agreement with the UAODS process at various temperatures, as shown in Table 3. In contrast, the pseudo-second-order model displayed much reduced correlation, particularly at the highest temperature (75 °C), deemed ideal, when R^2 plummeted to 0.96. The exceptionally high desulfurization efficiency (91% within 60 minutes) is the reason for the second-order model's failure at the high temperature (75 °C). The fast depletion of sulfur compounds at these high conversion levels causes nonlinear behavior in the second-order model, showing that the reaction follows a first-order model and that the concentration of sulfur in the fuel phase is the primary factor controlling the reaction rate. The ultrasonic cavity allows the reaction to continue even at very low concentrations and high temperatures by reducing the mass-transfer barrier between the bulk and the catalyst. As a result, a pseudo-first-order model was used to get the rate constant (k_1) and then use the Arrhenius equation to find the activation energy (Ea). The oxidant concentration remains relatively constant throughout the reaction compared to the sulfur concentration, which changes continuously over time. This makes the rate of reaction closely related to the sulfur concentration in the fuel, which in turn makes the reaction tend towards a pseudo-first-order kinetic model. As a result, pseudo-first-order kinetics may be used to crudely describe the response behavior. This behavior is comparable with what has been observed in ultrasonic-assisted oxidative desulfurization processes, where similar catalytic ODS systems have demonstrated strong agreement with the quasi-first-order kinetic model, indicating that this model is appropriate for the system under study. This is consistent with previous studies that confirm that the oxidation system follows Pesedo-first-order (Zahran et al., 2026; Zhang et al., 2016).

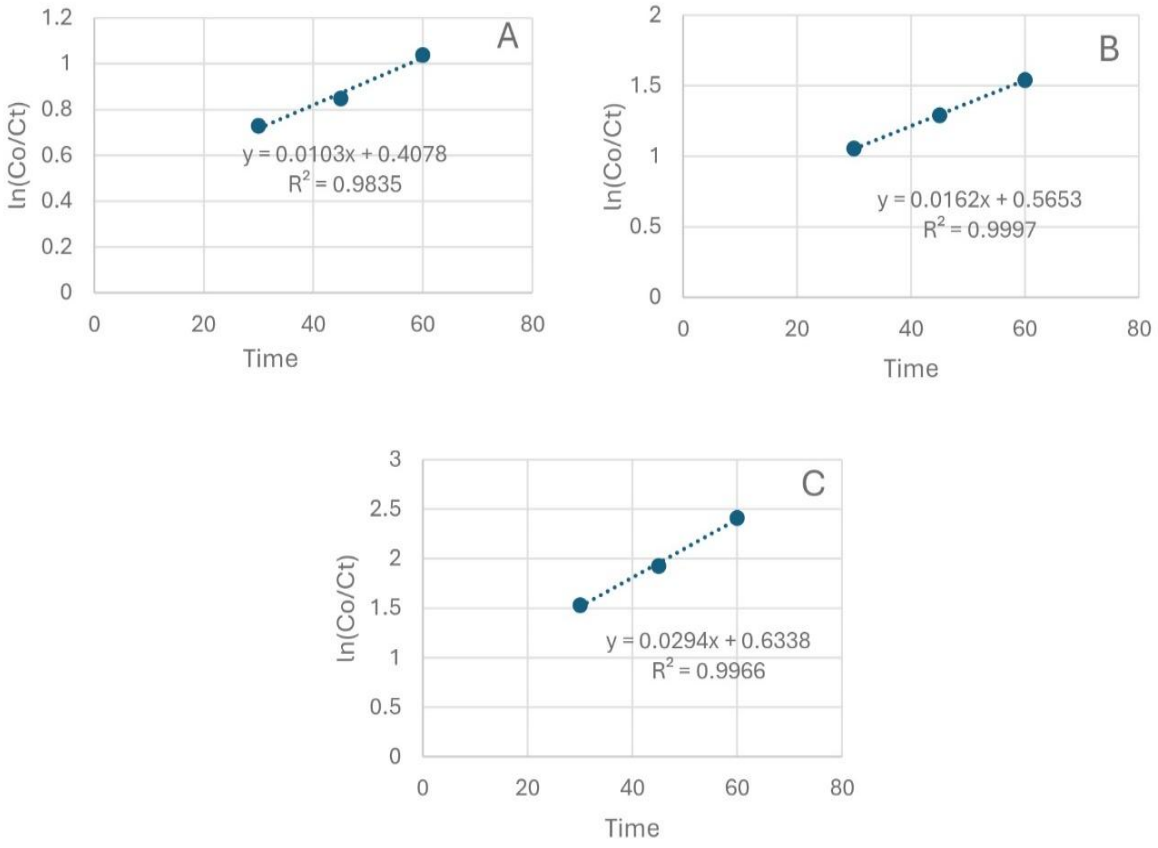

Figure 12. ln (Co/Ct) versus (t) of sulfur oxidation reactions using the prepared nano-catalyst (A) at 25 °C, (B) at 50 °C, (C) at 75 °C

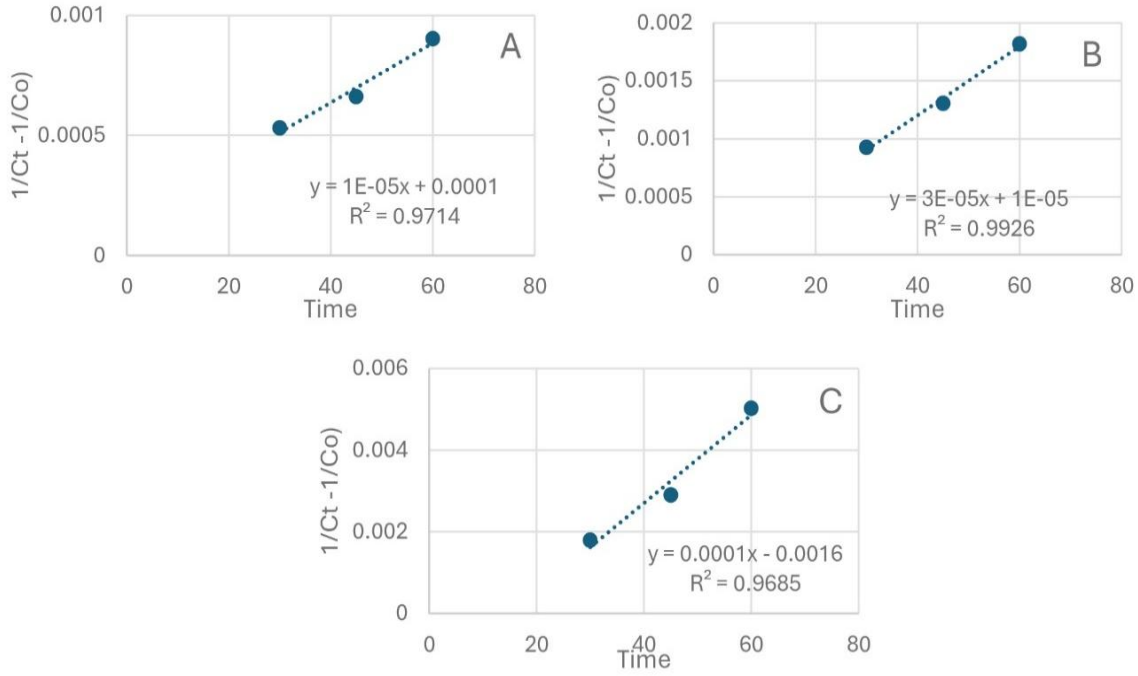

Figure 13. (1/Ct – 1/ Co) versus (t) of sulfur oxidation reactions using the prepared nano-catalyst (A) at 25 °C, (B) at 50 °C, (C) at 75 °

Table 3. Kinetic model results

Order of Reaction	K=constant	R^2
T= 25 °C		
The pseudo-first order	0.0103 (min^{-1})	0.9835
The pseudo-second order	$1*10^{-5}$ (ppm^{-1}. min^{-1})	0.9714
T= 50 °C		
The pseudo-first order	0.0162 (min^{-1})	0.99
The pseudo-second order	$1*10^{-4}$ (ppm^{-1}. min^{-1})	0.9926
T= 75 °C		
The pseudo-first order	0.0294 (min^{-1})	0.9966
The pseudo-second order	0.0004 (ppm^{-1}. min^{-1})	0.9685

Estimation of Activation Energy

Activation energy (Ea) calculations were carried out to examine the effectiveness of the generated nano-catalyst (Fe-Ni/γ-Al_2O_3) in the UAODS process. These computations examined how the reaction rate constant (k1) depended on temperatures (25, 50, and 75) using the linear Arrhenius equation (4):

$$lnk_1 = lnA - \frac{E_a}{RT} \dots\dots (4)$$

Where:

Ea: activation energy, R: gas constant, T: reaction temperature, A: pre-exponential factor.

The k1 vs 1/T graph in Fig.14 demonstrates a very linear relationship with a correlation coefficient (R^2) of 0.9849, demonstrating the validity of the kinetic data. According to the Arrhenius diagram's slope (-Ea/R), the activation energy was 18 kJ/mol, which is in line with the researchers' conclusions (Salih et al., 2026). The activation energy obtained in this study is consistent with previous studies, indicating that the applied model is suitable and that the oxidation reaction occurs at a low temperature. Furthermore, the ultrasonic waves contribute to increased mass transfer and contact between the reactants. The combined effect of iron and nickel may also contribute to a decrease in activation energy, which significantly increases the rate of sulfur removal. The unusually low value of Ea suggests that the energy barrier needed for the oxidation of sulfur compounds is greatly reduced by the synergistic combination of the active centers (iron and nickel) and ultrasonic cavitation (Gągol et al., 2019). This finding emphasizes how important ultrasonic waves are for improving the oil-oxidant phase contact, which speeds up the total rate of sulfur removal even at moderate temperatures.

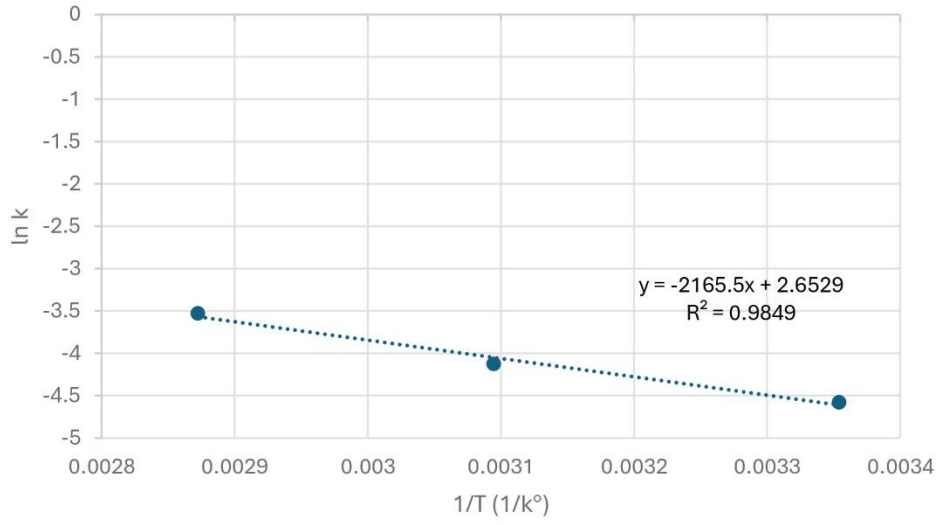

Figure 14. ln (K1) versus (1/T) of ODS reactions using the prepared nano-catalyst

Suggested Mechanism

The catalyst (Fe_2O_3 + NiO)/ γ-Al_2O_3 exhibits strong catalytic activity and 91% desulfurization efficiency due to dynamic chemical synergy between active iron and nickel sites. In Fenton-like oxidation processes, the reduction of iron (Fe^{+3}) to iron (Fe^{+2}) is the main and slowest barrier to the reaction rate. Here, nickel (Ni^{+2}) plays a critical synergistic function as an electron donor that speeds up the reduction of Fe^{+3} to Fe^{+2} throughout the double-cycle (Fe^{+3} + Ni^{+2}). The ferrous sites are constantly replenished by this quick reaction, which results in the very effective breakdown of hydrogen peroxide (H_2O_2) and the copious generation of active hydroxyl radicals (OH). The desulfurization rate is raised to levels much higher than those of traditional monometallic systems when this dual chemical synergy is coupled with the acoustic cavitation energy produced by ultrasonic waves, which prevents material agglomeration and removes oxidation products from the surface as they occur.

Fig.15 illustrates the reaction mechanism of ODS using a catalyst of (Fe_2O_3 + NiO)/ γ-Al_2O_3 and an oxidizing agent of H_2O_2. The reaction mechanism involves the transfer of sulfur compounds from diesel to the aqueous phase. This occurs through the adsorption of sulfur present in the diesel within the pores of (Fe_2O_3 + NiO)/ γ-Al_2O_3 or on the alumina surface, which is a good acid site for adsorbing sulfur compounds (Humadi et al., 2023b). Meanwhile, the metals (Ni/Fe) activate H_2O_2 on the catalyst surface. The oxidizing agent releases oxygen to oxidize the adsorbed sulfur and convert it into sulfoxides (Hossain et al., 2019). The oxidation process proceeds to create sulfones by adding another oxygen atom once a sulfoxide is formed. After being adsorbed onto the catalyst surface, these products move in the direction of the solid-liquid interface, where they are easier to separate from the system, specifically to the aqueous or organic phase. They have a higher molecular weight and higher boiling points than other sulfur compounds present in diesel, and are more polar, making them easier to remove using methods such as adsorption or extraction (Humadi et al., 2023b).

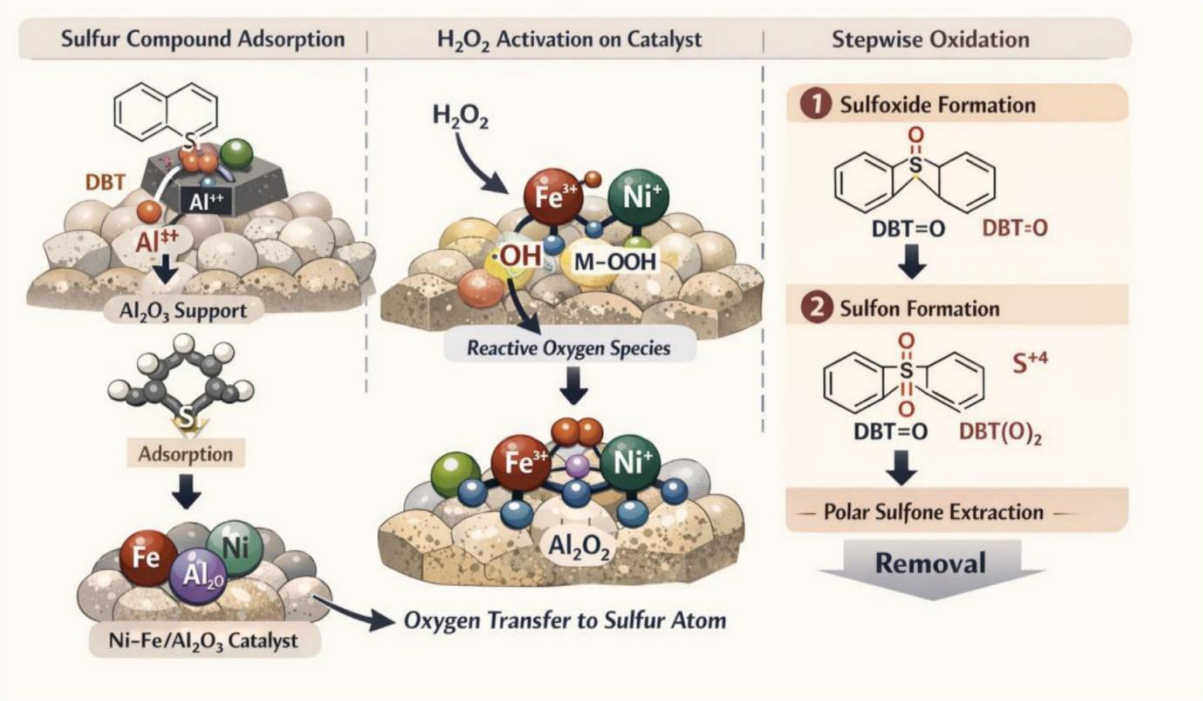

Figure 15: Suggested Mechanism of ODS with Heterogeneous Catalysts

The catalytic activity of the Fe_2O_3–NiO/γ-Al_2O_3 catalyst may be explained by the fact that the metallic sites help activate H_2O_2 and create reactive oxygen species that can oxidize sulfur compounds, depending on the kind of reaction system utilized. Iron actively contributes to the activation of H2O2 on the surface, which in turn contributes to the generation of active molecules such as hydroxyl radicals and other reactive oxygen species that effectively aid in oxidation processes (Li et al., 2023; Xu et al., 2024). Furthermore, electron transport and active site integration can be improved by adding a binary metal system, which contributes to increased removal efficiency and longer-lasting activation of hydrogen peroxide (H_2O_2) (Xu et al., 2024). Additionally, ultrasonic irradiation causes acoustic cavitation, which produces high-energy local conditions that speed up oxidative processes as well as concomitant physical and chemical effects such as improved mixing, emulsification, and mass transfer between phases (Ja'fari et al., 2018; Rajendran et al., 2020;

Albayrak and Tavman, 2022). In order to facilitate the oxidation of sulfur compounds and their transformation into more polar, removable products, the mechanism suggested in this work is based on the integration of H_2O_2 activation at the mineral sites and the improved effects of ultrasonic cavitation. This explanation is offered as a reactive mechanism that is compatible with the catalytic activity shown in the current investigation and backed by the published results and guiding principles of comparable systems.

Comparison of present and previous work

This research investigated the removal of sulfur compounds from diesel fuel using oxidative desulfurization technology on a large scale as an alternative to hydrodesulfurization. Many studies have used Al_2O_3-supported catalysts due to their high stability, large surface area, and ability to disperse and distribute the metals they support. Some of the studies that addressed this are shown in Table 4.

Table 4. Comparison of previous work

Fuel	catalyst	Sulfur Removal	Reference
Diesel	Co-Fe/γ-Al_2O_3	9.8%	(Yandy et al., 2023)
Diesel	AM/ Al_2O_3	54.63%	(García-Gutiérrez et al., 2014)
Diesel	PA/ Al_2O_3	55.95%	(García-Gutiérrez et al., 2014)
Diesel	MoO_3/Al_2O_3	%76.1	(Wan Abdullah et al., 2015b)
Diesel	Fe–MoO_3/Al_2O_3	%80	(Wan Abdullah et al., 2015a)
Diesel	MoO_3/Al_2O_3	43%	(Sundararaman and Song, 2014)

Reducing the sulfur concentration from 2018.14 ppm to about 180 ppm in the present processing step did not, by itself, satisfy the sulfur limitations for ultra-low sulfur gasoline, even though the desulfurization efficiency achieved 91% under ideal circumstances. However, the nature of the ODS technique employed in this investigation should be taken into consideration when interpreting this outcome. In order to separate the more polar oxidized sulfur compounds from the hydrocarbon phase, an ethanol extraction step comes after the desulfurization process, which does not just rely on oxidation. During the processing process, it was found that the production of sulfoxides and sulfones increases the polarity of the sulfur compounds and increases their likelihood of migrating to the polar phase during extraction, which directly lowers the amount of residual sulfur in the diesel. Therefore, a feasible strategy to further enhance the total removal of sulfur may be to raise the extraction efficiency or repeat the extraction process after oxidation. When further lower sulfur levels are needed, this might also be used in conjunction with subsequent oxidation-extraction processes. However, more research is needed to determine the ideal number of oxidation and extraction cycles needed to meet commercial fuel specifications, so the current findings are only a first step in evaluating the catalytic system's efficacy and the potential for expanding it into a multi-stage process.

4. CONCLUSION

Oxidative desulfurization (ODS) of sulfur compounds in diesel was performed using an ultrasonic reactor to test the performance of a prepared catalyst (Fe_2O_3 + NiO)/γ-Al_2O_3. Sonication intensities of 80%, 90%, and 100% were used at different temperatures (25–75°C) and reaction times (30–60 minutes) with the catalyst (Fe_2O_3 + NiO)/ γ-Al_2O_3, using the oxidizing agent H_2O_2 and a pressure of 1 atmosphere. The oxidative desulfurization process became much more efficient when ultrasound was used. By creating a lot of bubbles, the ultrasonic probe enhanced contact and mass transfer between the system components, improving the dispersion and mixing of the reaction components. The oxidative desulfurization procedure was more effective as a result of this effect. Following ethanol extraction, the desulfurization rate was 91% at 75°C and 60 minutes of reaction time, with 100% mixing efficiency.

The current catalytic system demonstrates good efficiency in removing sulfur compounds. Current work focuses on studying the prepared catalyst under operating and kinetic conditions, but the reuse of the catalyst during reaction cycles and the durability of the

solid material have not received sufficient attention in this study. These aspects are subject to review in future studies before moving to industrial applications.

Acknowledgement
The researcher would like to express his gratitude to Tikrit University and the College of Petroleum Process Engineering for lending their labs and providing the resources needed to carry out the practical and experimental portion of this work.

Author Contributions
Mohammad Kamal Saleh: Conceptualization, Methodology, Software, Investigation, Data curation, Writing - original draft, Writing - review & editing. Ghassan Hassan: Supervision. Jasim Ibrahim: Methodology, Writing - review & editing.

Ethical issues
Not applicable. This study does not involve any experiments on humans or animals. Hence, ethical approval was not required.

Informed consent
Not applicable.

Funding
This research did not receive any external funding like specific grant from funding agencies in the public, commercial, or nonprofit sectors.

Conflict of Interest
The authors declare that they have no conflicts of interest, competing financial interests or personal relationships that could have influenced the work reported in this paper.

Data and materials availability
All data and materials related to this study are available within the current manuscript.

REFERENCES

1. Aabid AA, Humadi JI, Ahmed GS, Jarullah AT, Ahmed MA, Abdullah WS. Enhancement of desulfurization process for light gas oil using new zinc oxide loaded over alumina nanocatalyst. Appl Sci Eng Prog 2023;16(3). doi:10.14416/j.asep.2023.02.007.
2. Abdulateef LT, Nawaf AT, Mahmood QA, Dahham OS, Noriman NZ, Shayfull Z. Preparation, characterization and application of alumina nanoparticles with multiple active component for oxidation desulfurization. AIP Conf Proc 2018;2030:020031. doi:10.1063/1.5066672.
3. Ahmed GS, Jarullah AT, Al-Tabbakh BA, Mujtaba IM. Design of an environmentally friendly reactor for naphtha oxidative desulfurization by air employing a new synthetic nano-catalyst based on experiments and modelling. J Clean Prod 2020;257:120436. doi:10.1016/j.jclepro.2020.120436.
4. Ahmed MJK, Ahmaruzzaman M. Adsorptive desulfurization of feed diesel using chemically impregnated coconut coir waste. Int J Environ Sci Technol 2015;12(9):2847-2856. doi:10.1007/s13762-014-0654-4.
5. Al-Tabbakh BA, Jarullah AT. Effect of calcination temperature on prepared Γ-Al2O3 as support catalyst. J Pet Res Stud 2023;13(3):74-90. doi:10.52716/jprs.v13i3.616.
6. Albayrak AT, Tavman A. Sono-oxidative desulfurization of fuels using heterogeneous and homogeneous catalysts: a comprehensive review. Ultrason Sonochem 2022;83:105845. doi:10.1016/j.ultsonch.2021.105845.
7. Algawi RJ, Humadi JI, Khamees LA. Experimental study of the impact of metal (iron, copper and aluminum) surface and light exposure on gum formation in Iraqi automotive gasoline. Pet Sci Technol 2024;42(21):2933-2944. doi:10.1080/10916466.2023.2179636.
8. Alwan HH, Ali AA, Makki HF. Optimization of oxidative desulfurization reaction with Fe2O3 catalyst supported on graphene using Box-Behnken experimental method. Bull Chem React Eng Catal 2020;15(1):175-185. doi:10.9767/bcrec.15.1.6670.175-185.
9. Barilla GRH, Chen CAW, Valencia MZM, Dugos NP, Choi AES. Mixing assisted oxidative desulfurization using a

synthesized catalyst of the activated carbon supported phosphotungstic acid: a process optimization study. S Afr J Chem Eng 2022;42:61-71. doi:10.1016/j.sajce.2022.06.012.

10. Beshkoofeh S, Ghalami-Choobar B, Shahidian Z, Khosharay S. Preparation, characterization, and kinetics model of MoCo/γ-Al2O3 catalysts for oxidative desulfurization of light naphtha. Iran J Chem Chem Eng 2021;40(6):1777-1792. doi:10.30492/ijcce.2020.127829.4161.
11. Beshtar M, Larimi A, Asgharinezhad AA. Enhanced super-ultra-deep photocatalytic oxidative desulfurization by titanium-activated metal-organic frameworks nanophotocataltyst. J Photochem Photobiol A Chem 2025;459:116056. doi:10.1016/j.jphotochem.2024.116056.
12. Bhasarkar JB, Dikshit PK, Moholkar VS. Ultrasound assisted biodesulfurization of liquid fuel using free and immobilized cells of Rhodococcus rhodochrous MTCC 3552: a mechanistic investigation. Bioresour Technol 2015;187:369-378. doi:10.1016/j.biortech.2015.03.102.
13. Cedeno-Caero L, Gomez-Bernal H, Fraustro-Cuevas A, Guerra-Gomez HD, Pedraza-Segura F. Oxidative desulfurization of synthetic diesel using supported catalysts: Part III. Support effect on vanadium-based catalysts. Catal Today 2008;133:244-254. doi:10.1016/j.cattod.2007.12.017.
14. Chica A, Corma A, Dómine ME. Catalytic oxidative desulfurization (ODS) of diesel fuel on a continuous fixed-bed reactor. J Catal 2006;242(2):299-308. doi:10.1016/j.jcat.2006.06.013.
15. Davoodi-Dehaghani F, Vosoughi M, Ziaee AA. Biodesulfurization of dibenzothiophene by a newly isolated Rhodococcus erythropolis strain. Bioresour Technol 2010;101(3):1102-1105. doi:10.1016/j.biortech.2009.08.058.
16. Dinamarca MA, Ibacache-Quiroga C, Baeza P, Galvez S, Villarroel M, Olivero P, Ojeda J. Biodesulfurization of gas oil using inorganic supports biomodified with metabolically active cells immobilized by adsorption. Bioresour Technol 2010;101(7):2375-2378. doi:10.1016/j.biortech.2009.11.086.
17. Fathi MI, Humadi JI, Mahmood QA, Talal A. Improvement of design synthetic nano-catalysts for performance enhancement of oxidative desulfurization using batch reactor. AIP Conf Proc 2022;2660:020026. doi:10.1063/5.0109089.
18. Gągol M, Darvishi Cheshmeh Soltani R, Przyjazny A, Boczkaj G. Effective degradation of sulfide ions and organic sulfides in cavitation-based advanced oxidation processes (AOPs). Ultrason Sonochem 2019;58:104610. doi:10.1016/j.ultsonch.2019.05.027.
19. García-Gutiérrez JL, Fuentes GA, Hernández-Terán ME, García-Gutiérrez P, Gutiérrez-Alejandre A, Murrieta F. Oxidative desulfurization of diesel using promising heterogeneous tungsten catalysts and hydrogen peroxide. Fuel 2014;138:118-125. doi:10.1016/j.fuel.2014.07.049.
20. Haruna A, Merican ZMA, Juma AK, Aliero AS, Ekeoma BC, Abdullahi M, Imam M, Abdulsalam S, Hamza SA. Fuel desulfurization using ionic liquids –An updated review. J Ionic Liq 2025;5(2):100162. doi:10.1016/j.jil.2025.100162.
21. Hossain MN, Park HC, Choi HS. A comprehensive review on catalytic oxidative desulfurization of liquid fuel oil. Catalysts 2019;9(3):229. doi:10.3390/catal9030229.
22. Hosseini SY, Khosravi Nikou MR. Synthesis and characterization of different γ-Al2O3 nanocatalysts for methanol dehydration to dimethyl ether. Int J Chem React Eng 2012;10(1).
23. Huang P, Luo G, Kang L, Zhu M, Dai B. Preparation, characterization and catalytic performance of HPW/aEVM catalyst on oxidative desulfurization. RSC Adv 2017;7(8):4681-4687. doi:10.1039/C6RA26587A.
24. Humadi JI, Nawaf AT, Jarullah AT, Ahmed MA, Hameed SA, Mujtaba IM. Design of new nano-catalysts and digital basket reactor for oxidative desulfurization of fuel: Experiments and modelling. Chem Eng Res Des 2023;190:634-650. doi:10.1016/j.cherd.2022.12.043.
25. Humadi JI, Issa YS, Aqar DY, Ahmed MA, Ali Alak HH, Mujtaba IM. Evaluation the performance of the tin (IV) oxide (SnO2) in the removal of sulfur compounds via oxidative-extractive desulfurization process for production an eco-friendly fuel. Int J Chem React Eng 2023;21(6):727-741. doi:10.1515/ijcre-2022-0046.
26. Ishihara A, Wang D, Dumeignil F, Amano H, Qian EW, Kabe T. Oxidative desulfurization and denitrogenation of a light gas oil using an oxidation/adsorption continuous flow process. Appl Catal A Gen 2005;279(1-2):279-287. doi:10.1016/j.apcata.2004.10.037.
27. Ja'fari M, Ebrahimi SL, Khosravi-Nikou MR. Ultrasound-assisted oxidative desulfurization and denitrogenation of liquid hydrocarbon fuels: A critical review. Ultrason Sonochem 2018;40:955-968. doi:10.1016/j.ultsonch.2017.09.002.
28. Jafar SA, Nawaf AT, Humadi JI. Improving the extraction of sulfur-containing compounds from fuel using surfactant material in a digital baffle reactor. Mater Today Proc 2021;42:1777-1783. doi:10.1016/j.matpr.2020.11.821.
29. Jarullah AT, Aldulaimi SK, Al-Tabbakh BA, Mujtaba IM. A new synthetic composite nano-catalyst achieving an environmentally friendly fuel by batch oxidative desulfurization. Chem Eng Res Des 2020;160:405-416. doi:10.1016/j.cherd.2020.05.015.
30. Jarullah AT, Al-Tabbakh BA, Ahmed MA, Hameed SA, Mujtaba IM. Design of Novel Synthetic Iron Oxide Nano-

Catalyst over Homemade Nano-Alumina for an Environmentally Friendly Fuel: Experiments and Modelling. Pet Coal 2022;64(4):917-937.
31. Jia Y, Li G, Ning G. Efficient oxidative desulfurization (ODS) of model fuel with H2O2 catalyzed by MoO3/γ-Al2O3 under mild and solvent free conditions. Fuel Process Technol 2011;92(1):106-111. doi:10.1016/j.fuproc.2010.09.011.
32. Jiang Z, Liu Y, Sun X, Tian F, Sun F, Liang C, You W, Han C, Li C. Activated carbons chemically modified by concentrated H2SO4 for the adsorption of the pollutants from wastewater and the dibenzothiophene from fuel oils. Langmuir 2003;19(3):731-736. doi:10.1021/la020670d.
33. Kayedi N, Samimi A, Asgari Bajgirani M, Bozorgian A. Enhanced oxidative desulfurization of model fuel: A comprehensive experimental study. S Afr J Chem Eng 2021;35:153-158. doi:10.1016/j.sajce.2020.09.001.
34. Khazaei A, Nazari S, Karimi G, Ghaderi E, Mansouri Moradian K, Bagherpor Z, Nazari S. Synthesis and characterization of γ-alumina porous nanoparticles from sodium aluminate liquor with two different surfactants. Int J Nanosci Nanotechnol 2016;12(4):207-214.
35. Kozerozhets IV, Panasyuk GP, Semenov EA, Avdeeva VV, Danchevskaya MN, Simonenko NP, Vasiliev MG, Kozlova LO, Ivakin YD. State and forms of water in dispersed aluminum oxides and hydroxides. Ceram Int 2023;49(18):30381-30394. doi:10.1016/j.ceramint.2023.06.300.
36. Li L, Yin Z, Cheng M, Qin L, Liu S, Yi H, Zhang M, Fu Y, Yang X, Zhou X, Zeng G, Lai C. Insights into reactive species generation and organics selective degradation in Fe-based heterogeneous Fenton-like systems: a critical review. Chem Eng J 2023;454:140126. doi:10.1016/j.cej.2022.140126.
37. Ludwig B, Burke TT. Infrared spectroscopy studies of aluminum oxide and metallic aluminum powders, Part I: thermal dehydration and decomposition. Powders 2022;1(1): 47-61. doi:10.3390/powders1010005.
38. de Luna MDG, Futalan CM, Dayrit RA, Choi AES, Wan MW. Evaluation of continuously mixed reactor configurations in the oxidative-adsorptive desulfurization of diesel fuel: optimization and parametric studies. J Clean Prod 2018;203: 664-673. doi:10.1016/j.jclepro.2018.08.287.
39. Ma Y, Tang F, Liu Z, Li J, Wang H, Wu F, Wang D, Lu AH. A thermodynamic model of the surface hydroxylation of γ-Al2O3. Phys Chem Chem Phys 2024;26(28):19543-19553. doi: 10.1039/D4CP01968G.
40. Mangesh VL, Govindarajan M, Chekuri RBR, Perumal T, Rajendran K, Chandrasekaran K, Kumar NS, Basivi PK, Alreshaidan SB, Al-Fatesh AS. Ni–Fe bimetallic catalysts with high dispersion supported by SBA-15 evaluated for the selective oxidation of benzyl alcohol to benzaldehyde. RSC Adv 2024;14(4):2300-2310. doi:10.1039/D3RA07086G.
41. Martín N, Cirujano FG, García-Verdugo E, Llorca J, del Río E, Jiménez-Morales I, Bogeat-Barroso A, López-Maya E, Álvarez MG. Tuning Ni-pyrazolate frameworks by post-synthetic Fe-incorporation for oxidase-mimicking H2O2 activation. ChemPlusChem 2023;88(12):e202300447. doi:10.1002/cplu.2023 00447.
42. Miao G, Ye FY, Wu LM, Ren XL, Xiao J, Li Z, Wang HH. Selective adsorption of thiophenic compounds from fuel over TiO2/SiO2 under UV-irradiation. J Hazard Mater 2015;300: 426-432. doi:10.1016/j.jhazmat.2015.07.027.
43. Mohammed AE, Mohammed WT, Gheni SA. Scale-up of oxidative desulfurization for sour diesel fuel: modeling, simulation, and reactor design using Fe/AC catalyst. Case Stud Chem Environ Eng 2025;11:101024. doi:10.1016/j.cscee. 2024.101024.
44. Mohammed HJ, Jarullah AT. Experimental design of oxidative desulfurization of kerosene through response surface methodology (RSM). Tikrit J Eng Sci 2023;30(2):130-141. doi: 10.25130/tjes.30.2.14.
45. Mohammed WT, Almilly RFK, Al-Ali SBA. Desulfurization of diesel fuel by oxidation and solvent extraction. J Eng 2015;21(2):87-102. doi:10.31026/j.eng.2015.02.06.
46. Nawaf AT, Jarullah AT, Hameed SA, Mujtaba IM. Design of new activated carbon-based adsorbents for improved desulfurization of heavy gas oil: experiments and kinetic modeling. Chem Prod Process Model 2021;16(3):229-249. doi:10.1515/cppm-2020-0107.
47. Nawaf AT, Jarullah AT, Abdulateef LT. Design of a synthetic zinc oxide catalyst over nano-alumina for sulfur removal by air in a batch reactor. Bull Chem React Eng Catal 2019;14(1): 79-92. doi:10.9767/bcrec.14.1.2507.79-92.
48. Özcan O, Akın AN. Organic and inorganic sol-gel routes for preparing mesoporous γ-alumina powder. Gazi Univ J Sci 2025;38(4):1703-1719. doi:10.35378/gujs.1521093.
49. Rajendran A, Cui T, Fan H, Yang Z, Feng J, Li W. A comprehensive review on oxidative desulfurization catalysts targeting clean energy and environment. J Mater Chem A 2020;8(5):2246-2285. doi:10.1039/C9TA12555H.
50. Sundararaman R, Song C. Catalytic oxidative desulfurization of diesel fuels using air in a two-step approach. Ind Eng Chem Res 2014;53(5):1890-1899. doi:10.1021/ie403445f.
51. Rayalu SS, Udhoji JS, Meshram SU, Naidu RR, Devotta S. Estimation of crystallinity in flyash-based zeolite-A using XRD and IR spectroscopy. Curr Sci 2005;89(12):2147-2151.
52. Razzaq GHA, Hamad KI, Humadi JI. Silver nanoparticles for ultrasonic assisted synthesis of oxidant agents in micro-

reactor: kinetic analysis and process intensification. Mater Sci Forum 2023;1083:23-32. doi:10.4028/p-0brrx7.

53. Salem HM, Hassan MA, Ahmed KF, Mohamed AA. Review in desulfurization of liquid fuels: microwave and ultrasound oxidative-assisted techniques. Fuel 2025;401:135862. doi: 10.1016/j.fuel.2025.135862.
54. Salih MK, AbdulRazzaq GH, Humadi JI. Studying the effect of different parameters on the oxidation desulfurization of diesel fuel using Fe2O3-NiO/SiO2 bimetallic catalyst: experimental and kinetic models. Iraqi J Chem Pet Eng 2026;27(2):155-171. doi:10.31699/IJCPE.2026.2.12.
55. Sobhani M, Tavakoli H. The effect of cobalt addition on the meso-porous structured γ-alumina synthesized by aqueous sol-gel method. J Ultrafine Grained Nanostruct Mater 2019;52(1):84-89. doi:10.22059/JUFGNSM.2019.01.09.
56. Tavan Y, Shahrokhi M, Farhadi F. Electrochemical oxidative desulfurization for high sulfur content crude gas-oil. Sep Purif Technol 2020;248:117117. doi:10.1016/j.seppur.2020.117117.
57. Wan Abdullah WN, Wan Abu Bakar WA, Ali R, Embong Z. Oxidative desulfurization of commercial diesel catalyzed by tert-butyl hydroperoxide polymolybdate on alumina: optimization by Box-Behnken design. Clean Technol Environ Policy 2015;17(2):433-441. doi:10.1007/s10098-014-0797-5.
58. Wan Abdullah WN, Wan Abu Bakar WA, Ali R. Alumina supported polymolybdate catalysts utilizing tert-butyl hydroperoxide oxidant for desulfurization of Malaysian diesel fuel. Korean J Chem Eng 2015;32(10):1999-2006. doi:10.1007/s11814-015-0047-5.
59. Wang H, Gao Z, Sun B, Mu S, Dang F, Guo X, Ma D, Shi C. Engineering metal-support interaction to construct catalytic interfaces and redisperse metal nanoparticles. Chem Catal 2023;3(10):100768. doi:10.1016/j.checat.2023.100768.
60. Wu F, Yuan Q, Wang J, Wang X, Luo J, Guo Y, Xu H, Wei X. Oxidative desulfurization catalyzed by magnetically recoverable CoFe2O4 nano-particles. Arab J Chem 2025;18(1): 106076. doi:10.1016/j.arabjc.2024.106076.
61. Xu G, Liu Q, Mai Z, Wang M, Zhao H, Xu K. Strategies for improving performance of iron-based catalysts in activating heterogeneous Fenton-like oxidation in pollutants degradation: from the perspective of materials structure design. Process Saf Environ Prot 2024;190:794-820. doi:10.1016/j.psep.2024.08.082.
62. Yandy Y, Widyasari NF, Berliana T, Nasikin M. Heterogeneous catalyst of oxidative desulfurization for reducing sulfur content in Indonesia Biosolar. In: Proceedings 4th Int Conf Chem Eng App Sci 2023. doi:10.5220/0011811800003575.
63. Ye Q, Hunter TN, Xu H, Harbottle D, Kale GM, Tillotson MR. Synergistic effect of Fe and Ni on carbon aerogel for enhanced oxygen reduction and H2O2 activation in electro-Fenton process. Sep Purif Technol 2025;353:128436. doi: 10.1016/j.seppur.2024.128436.
64. Zahran AI, El-Fawal EM, El Naggar AMA, Hassanein TF. Production of low sulfur diesel fuel through ultrasonic catalytic oxidative route using novel mixed oxides nanocomposites assisted by solvent extraction. Sci Rep 2026;16(1):12058. doi:10.1038/s41598-026-39220-0.
65. Zeifert BH, Salmones J, Hernández JA, Reynoso R, Nava N, Reguera E, Cabañas-Moreno JG, Aguilar-Ríos G. X-ray diffraction and Mössbauer characterization of Raney Fe-Ni catalysts. J Radioanal Nucl Chem 2000;245(3):637-639. doi:10.1023/A:1006798302775.
66. Zhang G, Yu F, Wang R. Research advances in oxidative desulfurization technologies for the production of low sulfur fuel oils. Pet Coal 2009;51(3):196-207. No DOI verified.
67. Zhang X, Zhu Y, Huang P, Zhu M. Phosphotungstic acid on zirconia-modified silica as catalyst for oxidative desulfurization. RSC Adv 2016;6(73):69357-69364. doi:10.1039/C6RA16622A.
68. Zuraiqi K, Nancarrow P, Ahmed H. Ultrasound and ionic liquid-enhanced extractive desulfurization of diesel. MATEC Web Conf 2018;171:03003. doi:10.1051/matecconf/201817103003.